Computer Physics Communications 326 (2026) 110209

Contents lists available at ScienceDirect

Computer Physics Communications

journal homepage: www.elsevier.com/locate/cpc

New Version Announcement

C++ CUDA programs for solving the time-dependent dipolar Gross-Pitaevskii equation

Denis Mujo [a], Dušan Vudragović [a,*], Paulsamy Muruganandam [b,c], Sadhan K. Adhikari [d]

[a] Scientific Computing Laboratory, Center for the Study of Complex Systems, Institute of Physics Belgrade, University of Belgrade, Pregrevica 118, Belgrade, 11080, Serbia
[b] Department of Physics, Bharathidasan University, Tiruchirappalli, Tamil Nadu, 620024, India
[c] Department of Medical Physics, Bharathidasan University, Tiruchirappalli, Tamil Nadu, 620024, India
[d] Instituto de Física Teórica, UNESP – Universidade Estadual Paulista, 01.140-70 São Paulo, São Paulo, Brazil

ARTICLE INFO

The review of this paper was arranged by Prof. Dr. J Ballantyne

PACS:
02.60.Cb
02.60.Lj
02.60.Jh
02.60.Cb
03.75.-b
67.85.-d

Keywords:
Bose-Einstein condensate
Gross-Pitaevskii equation
Dipolar atoms
Quantum fluctuations
Quantum droplets
Split-step Crank-Nicolson scheme
Real- and imaginary-time propagation
Partial differential equation
C++ program
CUDA program
GPU

ABSTRACT

This paper introduces an improved version of our previous CUDA programs [1] for solving the dipolar Gross-Pitaevskii equation in three spatial dimensions, now incorporating a quantum fluctuation term [2–4]. This enhancement is vital for accurately modeling quantum dipolar droplets [5,6] in dipolar Bose-Einstein condensates. Originally developed in C, the code has been transitioned to C++ to take advantage of its features. Speedup tests were conducted on two types of GPU cards – one commercial and one HPC-optimized – and the results were compared to earlier versions on GPUs and a modern HPC cluster. Both configurations showed an increase in speed.

NEW VERSION PROGRAM SUMMARY

Program title: DBEC-GP-CUDA package, consisting of: (i) imag3d-cuda, (ii) real3d-cuda.
CPC Library link to program files: https://doi.org/10.17632/s858p8zsgp.2
Licensing provisions: CC by 4.0.
Programming language: OpenMP C++; CUDA C++.
Supplementary material: 10.1016/j.cpc.2026.110209.
Journal reference of previous version: Comput. Phys. Commun. 200 (2016) 406.
Does the new version supersede the previous version?: No.

Nature of problem: These programs are developed to solve the time-dependent nonlinear Gross-Pitaevskii equation (GPE), including contact and dipolar interactions, as well as a quantum fluctuations term [2,3]. within an anisotropic harmonic trap. The package offers programs for solving GPE in three spatial dimensions, capable of computing both stationary and non-stationary solutions through imaginary or real-time propagation.

Solution method: The time-dependent GPE is solved using the same split-step semi-implicit Crank-Nicolson method as before [7,8], enabling the calculation of stationary and non-stationary solutions through propagation in imaginary or real time. The dipolar interaction term is evaluated by applying a Fourier transform to momentum space using the convolution theorem. The quantum fluctuation term has an integral that can be calculated analytically, and therefore, we avoid doing numerical integration for that term.

Reasons for the new version: The development of the new code is motivated by two main reasons. First, the previous version lacked the quantum fluctuation term, which is crucial for accurately modeling stable quantum dipolar droplets. Without it, the code cannot simulate droplet formation, resulting in system collapse at the mean-field level due to predominantly attractive interactions. By adding this term, the system is mechanically stabilized against collapse, allowing the updated code to simulate the process correctly. And considering that the previous Fortran, C, and CUDA programs are widely used in the ultra-cold

* Corresponding author.
E-mail addresses: denis.mujo@ipb.ac.rs (D. Mujo), dusan.vudragovic@ipb.ac.rs (D. Vudragović), anand@bdu.ac.in (P. Muruganandam), adhikari@ift.unesp.br (S.K. Adhikari).

https://doi.org/10.1016/j.cpc.2026.110209
Received 30 March 2026; Received in revised form 27 April 2026; Accepted 5 May 2026
Available online 7 May 2026

atoms community [9–17] and with the discovery of quantum dipolar droplets, we have found it beneficial to have programs that can properly simulate them as well. Second, with modern computers typically equipped with GPUs and HPC clusters with even more powerful GPU cards, we made several improvements and optimizations to better utilize these resources. These enhancements boost performance on modern systems. On the NVIDIA A30 GPU, the speedup over previously published OpenMP/MPI-parallelized programs [18] running on 128 Intel Xeon Gold 6338 CPU cores is 3 or higher. Additionally, we converted the code from C to C++ to utilize standard library features and adopted an object-oriented approach, enhancing code abstraction and structure.

Summary of revisions: The revised code extends the original dipolar Gross–Pitaevskii programs [1] for solving the dipolar GPE by including the beyond-mean-field quantum fluctuation term needed to describe dipolar quantum droplets, as explained in the supplementary material. This additional contribution follows the formulation of Lima and Pelster [2,3] and is implemented in dimensionless form together with the contact and dipolar interactions.

As described in the supplementary material, this new term is incorporated into the non-derivative part of the propagation scheme through the existing `calcnu` routine. The implementation is validated with simulation examples for ^{164}Dy condensates, including imaginary-time ground-state calculations and real-time evolution after a quench into the dipole-dominated regime, where droplet formation is observed.

In addition to the physics extension, the supplementary material highlights several code improvements. The evolution procedure is simplified into a single main loop, new parameters (NITER, NSNAP, MUEND) improve monitoring and convergence control, and initialization is made more flexible through user-defined Gaussian widths and optional automatic grid-step selection. The revised programs also improve memory management and GPU execution, leading to measurable performance gains over previous CUDA versions and strong speedups compared with earlier implementations.

Additional comments including Restrictions and Unusual features: This package includes two programs: imag3d-cuda for imaginary time propagation and real3d-cuda for real time propagation. Programs are compatible with computers that have NVIDIA GPU cards with Compute Capability 6.0 or higher and require CUDA toolkit versions above 8.0. Because the FFT algorithm in the cuFFT library, our programs may consume varying amounts of memory depending on the grid sizes N_x, N_y, and N_z. For instance, if a grid size is a large prime number, cuFFT will employ an algorithm that requires significantly more memory - often several times more - compared to a grid size that is a power of two. Generally, smaller prime numbers lead to better performance, with the best results achieved when the grid size is a power of two.

CRediT authorship contribution statement

Denis Mujo: Writing – review & editing, Validation, Software, Investigation, Formal analysis; **Dušan Vudragović:** Writing – original draft, Visualization, Validation, Supervision, Software, Investigation, Conceptualization; **Paulsamy Muruganandam:** Writing – review & editing, Validation, Supervision, Software, Investigation, Conceptualization; **Sadhan K. Adhikari:** Writing – review & editing, Visualization, Validation, Supervision, Software, Investigation, Conceptualization.

Data availability

Codes are provided in the Attach Files step.

Declaration of competing interest

The authors declare that they have no known competing financial interests or personal relationships that could have appeared to influence the work reported in this paper.

Acknowledgements

D. M. and D. V. acknowledge support provided by the Institute of Physics Belgrade, through the grant by the Ministry of Science, Technological Development, and Innovations of the Republic of Serbia. The work of P. M. is supported by the Ministry of Education-Rashtriya Uchchatar Shiksha Abhiyan (MoE RUSA 2.0): Bharathidasan University–Physical Sciences. S. K. A. acknowledges support by the Conselho Nacional de Desenvolvimento Cient ífico e Tecnológico (Brazil) grant 303885/2024-6. Numerical simulations were run on the PARADOX supercomputing facility at the Scientific Computing Laboratory, National Center of Excellence for the Study of Complex Systems, Institute of Physics Belgrade.

Supplementary material

Supplementary material associated with this article can be found in the online version at 10.1016/j.cpc.2026.110209.

References

[1] V. Lončar, A. Balaž, A. Bogojević, S. Škrbić, P. Muruganandam, S.K. Adhikari, CUDA programs for solving the time-dependent dipolar Gross-Pitaevskii equation in an anisotropic trap, Comput. Phys. Commun. 200 (2016) 406–410. https://doi.org/10.1016/j.cpc.2015.11.014

[2] A.R.P. Lima, A. Pelster, Beyond mean-field low-lying excitations of dipolar Bose gases, Phys. Rev. A 86 (2012) 063609. https://doi.org/10.1103/PhysRevA.86.063609

[3] A.R.P. Lima, A. Pelster, Quantum fluctuations in dipolar Bose gases, Phys. Rev. A 84 (2011) 041604. https://doi.org/10.1103/PhysRevA.84.041604

[4] F. Wächtler, L. Santos, Quantum filaments in dipolar Bose-Einstein condensates, Phys. Rev. A 93 (2016) 061603. arXiv:1601.04501, https://doi.org/10.1103/PhysRevA.93.061603

[5] H. Kadau, M. Schmitt, M. Wenzel, C. Wink, T. Maier, I. Ferrier-Barbut, T. Pfau, Observing the Rosensweig instability of a quantum ferrofluid, Nature 530 (2016) 194–197. https://doi.org/10.1038/nature16485

[6] I. Ferrier-Barbut, H. Kadau, M. Schmitt, M. Wenzel, T. Pfau, Observation of quantum droplets in a strongly dipolar Bose gas, Phys. Rev. Lett. 116 (2016) 215301. https://doi.org/10.1103/PhysRevLett.116.215301

[7] P. Muruganandam, S.K. Adhikari, Fortran programs for the time-dependent Gross-Pitaevskii equation in a fully anisotropic trap, Comput. Phys. Commun. 180 (2009) 1888–1912. https://doi.org/10.1016/j.cpc.2009.04.015

[8] R.K. Kumar, L.E. Young-S., D. Vudragović, A. Balaž, P. Muruganandam, S.K. Adhikari, Fortran and C programs for the time-dependent dipolar Gross-Pitaevskii equation in an anisotropic trap, Comput. Phys. Commun. 195 (2015) 117–128. arXiv:1506.03283, https://doi.org/10.1016/j.cpc.2015.03.024

[9] S.K. Adhikari, Bright dipolar Bose-Einstein-condensate soliton mobile in a direction perpendicular to polarization, Phys. Rev. A 90 (2014) 055601. arXiv:1410.1369, https://doi.org/10.1103/PhysRevA.90.055601

[10] S.K. Adhikari, Stable matter-wave solitons in the vortex core of a uniform condensate, J. Phys. B At. Mol. Phys. 48 (2015) 165303. arXiv:1506.06367, https://doi.org/10.1088/0953-4075/48/16/165303

[11] S.K. Adhikari, Stable spatial and spatiotemporal optical soliton in the core of an optical vortex, Phys. Rev. E 92 (2015) 042926. arXiv:1510.03663, https://doi.org/10.1103/PhysRevE.92.042926

[12] H. Al-Jibbouri, I. Vidanović, A. Balaž, A. Pelster, Geometric resonances in Bose-Einstein condensates with two- and three-body interactions, J. Phys. B At. Mol. Phys. 46 (2013) 065303. arXiv:1208.0991, https://doi.org/10.1088/0953-4075/46/6/065303

[13] J. Akram, A. Pelster, Sculpting quasi-one-dimensional Bose-Einstein condensate to generate calibrated matter waves, Phys. Rev. A 93 (2016) 023606. arXiv:1509.03826, https://doi.org/10.1103/PhysRevA.93.023606

[14] T. Khellil, A. Balaž, A. Pelster, Analytical and numerical study of dirty bosons in a quasi-one-dimensional harmonic trap, New J. Phys. 18 (2016) 063003. arXiv:1510.04985, https://doi.org/10.1088/1367-2630/18/6/063003

[15] I. Vasić, A. Balaž, Excitation spectra of a Bose-Einstein condensate with an angular spin-orbit coupling, Phys. Rev. A 94 (2016) 033627. arXiv:1602.03538, https://doi.org/10.1103/PhysRevA.94.033627

[16] C.-Y. Lai, C.-C. Chien, Geometry-induced memory effects in isolated quantum systems: cold-atom applications, Phys. Rev. Appl. 5 (2016) 034001. arXiv:1510.08978, https://doi.org/10.1103/PhysRevApplied.5.034001

[17] P. Das, P.K. Panigrahi, Controlled generation of nonlinear resonances through sinusoidal lattice modes in Bose-Einstein condensate, Laser Phys. 25 (2015) 125501. arXiv:1506.00795, https://doi.org/10.1088/1054-660X/25/12/125501

[18] V. Lončar, L.E. Young-S., S. Škrbić, P. Muruganandam, S.K. Adhikari, A. Balaž, OpenMP, OpenMP/MPI, and CUDA/MPI C programs for solving the time-dependent dipolar Gross-Pitaevskii equation, Comput. Phys. Commun. 209 (2016) 190–196. arXiv:1610.05329, https://doi.org/10.1016/j.cpc.2016.07.029

Supplemental material: C++ CUDA programs for solving the time-dependent dipolar Gross-Pitaevskii equation

Denis Mujo[a], Dušan Vudragović[a,*], Paulsamy Muruganandam[b,c], Sadhan K. Adhikari[d]

[a] *Scientific Computing Laboratory, Center for the Study of Complex Systems, Institute of Physics Belgrade, University of Belgrade, Pregrevica 118, 11080 Belgrade, Serbia*
[b] *Department of Physics, Bharathidasan University, Tiruchirappalli 620024, Tamil Nadu, India*
[c] *Department of Medical Physics, Bharathidasan University, Tiruchirappalli 620024, Tamil Nadu, India*
[d] *Instituto de Física Teórica, UNESP – Universidade Estadual Paulista, 01.140-70 São Paulo, São Paulo, Brazil*

In dipolar Bose-Einstein condensates (BEC), mean-field interactions alone are insufficient to describe the emergence and stability of quantum droplets. To capture the crucial role of beyond-mean-field effects, the Gross-Pitaevskii equation (GPE) is extended by an additional term that incorporates the contribution of quantum fluctuations. This leads to the following extended GPE, which incorporates both mean-field dipolar interactions and the beyond-mean-field correction

$$i\frac{\partial\Psi}{\partial t} = \left(-\frac{1}{2}\nabla^2 + U + g|\Psi|^2 + g_{\rm dd}\int d^3r' \frac{1-3\cos^2\theta}{|\mathbf{r}-\mathbf{r}'|^3}|\Psi|^2 + h_2|\Psi|^3\right)\Psi, \tag{1}$$

where g and $g_{\rm dd}$ are, respectively, the contact and dipole-dipole interaction coupling constants with $g = 4\pi N a_s/\ell$ and $g_{\rm dd} = 3N a_{\rm dd}/\ell$, U is the trap potential, N is the number of atoms in the condensate, and h_2 represents the quantum fluctuations term [2, 3]. GPE Eq. (1) is expressed in dimensionless form and integrated into the code accordingly. This is accomplished by selecting a reference frequency ω_r and defining all other physical variables relative to it, i.e., lengths are measured in harmonic oscillator units $\ell = \sqrt{\hbar/(m\omega_r)}$, time in units of $1/\omega_r$, and energy in units of $\hbar\omega_r$. This extended formulation provides a quantitatively accurate description of both the formation and the equilibrium properties of dipolar quantum droplets.

The quantum fluctuation term in the code is derived from Lima and Pelster's research [2, 3], where they first formulated this term for dipolar Bose gases using Bogoliubov-de Gennes (BdG) theory. To extend beyond the mean-field approximation, we decomposed the field operator into the wave function around the condensate wave function, Ψ_c, including a term for quantum fluctuations $\delta\hat{\Psi}$, so that $\hat{\Psi} = \Psi_c + \delta\hat{\Psi}$, retaining terms up to second order in quantum fluctuations. These fluctuations result in a shift in the chemical potential, and BdG theory supplies the term to model this shift

$$h_2 = \frac{128\sqrt{\pi}}{3}\left(\frac{a_s}{\ell}\right)^{5/2} N^{3/2} Q_5,\ Q_5(\epsilon_{\rm dd}) = \int_0^1 du\left(1-\epsilon_{\rm dd}+3u^2\epsilon_{\rm dd}\right)^{5/2}, \tag{2}$$

where $\epsilon_{\rm dd} = a_{\rm dd}/a_s$ represents the relative interaction strength. The Q_5 term has an analytical expression, eliminating the need for numerical integration in our codes. For $\epsilon_{\rm dd} > 1$, which is the section where quantum droplets may form, the Q_5 term gains an imaginary component as well. However, this imaginary part is significantly smaller than the real part, as illustrated in Figure 1, and can be neglected [19, 20].

As seen in Eq. (1), the quantum fluctuation term does not depend on spatial derivatives. Therefore, it is incorporated into our program as an additional term within the `calcnu` function, which handles time propagation for the Hamiltonian component without spatial derivatives.

Figure 2 presents the simulation results based on the input parameters from the experimental setup [5] to demonstrate the code's functionality. On the left, the figure shows the ground-state condensate density $n(x,y) = \int dz|\Psi(x,y,z)|^2$, resulting from the imaginary-time propagation of $N = 20000$ ^{164}Dy atoms, with the contact and dipole-dipole interaction strengths set to $a_s = a_{\rm dd} = 132\,a_0$ (where a_0 is Bohr radius), which aligns with the experimental conditions. The system's real-time dynamics are simulated by applying a quench to the contact interaction strength, reducing it to $a_s = 80\,a_0$. This moves the system into the dipole-dominated regime $\epsilon_{\rm dd} > 1$, which is essential for quantum droplet formation. The right side of the Figure 2 shows the condensate density after 110 ms, where droplet formation is clearly visible.

*Corresponding author.
Email addresses: `denis.mujo@ipb.ac.rs` (Denis Mujo), `dusan.vudragovic@ipb.ac.rs` (Dušan Vudragović), `anand@bdu.ac.in` (Paulsamy Muruganandam), `adhikari@ift.unesp.br` (Sadhan K. Adhikari)

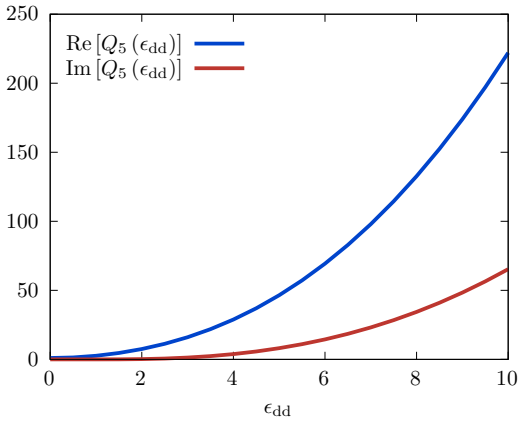

Figure 1: Real and imaginary parts of Q_5 integral as functions of the relative interaction strength, ϵ_{dd}. Notably, the imaginary part is much smaller than the real part, highlighting the dominance of the real component for different ϵ_{dd} values.

When initialized in a droplet configuration, the condensate preserves its structure during real-time evolution if the state corresponds to a stable solution of the extended GPE. In such cases, the density profile remains essentially unchanged, apart from minor numerical fluctuations or weak collective excitations, confirming that the droplet arrangement represents a stationary or long-lived metastable state. This behavior is illustrated in Figure 3, where the droplet pattern obtained via imaginary-time propagation (a) is used as the initial condition for real-time evolution. As shown in Figure 3 (b), the integrated quasi-2D density at $t = 10\,\text{ms}$ retains the same spatial structure, demonstrating the dynamical stability of the droplet configuration for the chosen parameters ($N = 80000$, $a = 85\,a_0$, $a_{dd} = 130.8\,a_0$).

In the updated code, we've also revised the main evolution loop. Previously, the program used three separate conditional loops—one to introduce the nonlinearities for contact and dipolar interaction, the second to run with fixed nonlinearities, and the third for the final run with fixed nonlinearities. The updated version features a single loop that includes fixed nonlinearities.

The updated code enhances simulation progress monitoring. Unlike the previous version, where physical quantities were calculated only after each main loop, the new version introduces configurable options using the NITER and NSNAP variables. NITER sets the total number of iterations, while NSNAP determines how many snapshots are taken, i.e., how often the physical quantities are calculated during the NITER iterations. To remain compatible with the outputs of the previous code version, one can set NSNAP to 1 to produce the same output.

The updated code now terminates the simulation conditionally once the chemical potential reaches stability. A new optional configuration parameter, MUEND, has been introduced to specify the permissible relative deviation of the chemical potential between two consecutive time steps. When MUEND is set, the simulation will run until the condition $|\mu_{i-1} - \mu_i|/\mu_i >$ MUEND is satisfied, where μ_{i-1} and μ_i are

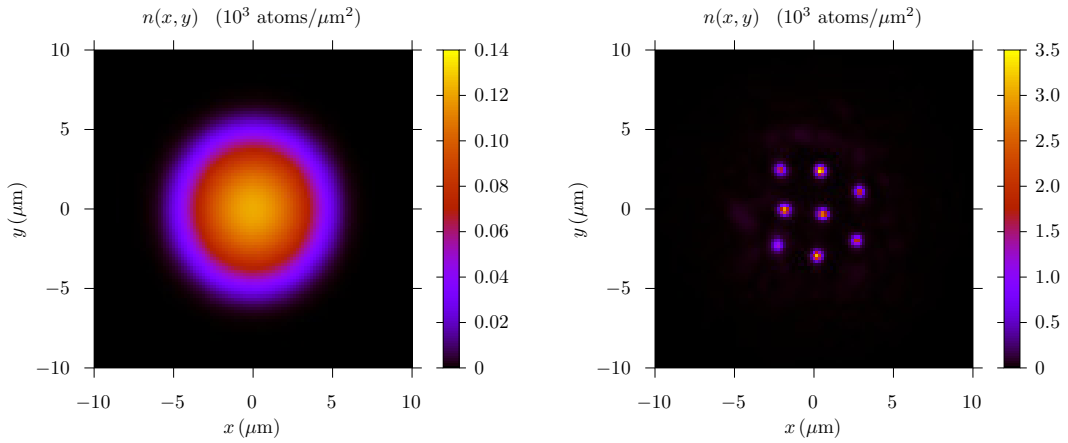

Figure 2: Ground-state condensate densities $n(x, y)$ are shown after imaginary-time propagation (left) and after 110 ms of real-time propagation (right), following a quench in contact interaction strength from $a_s = 132\,a_0$ to $a_s = 80\,a_0$.

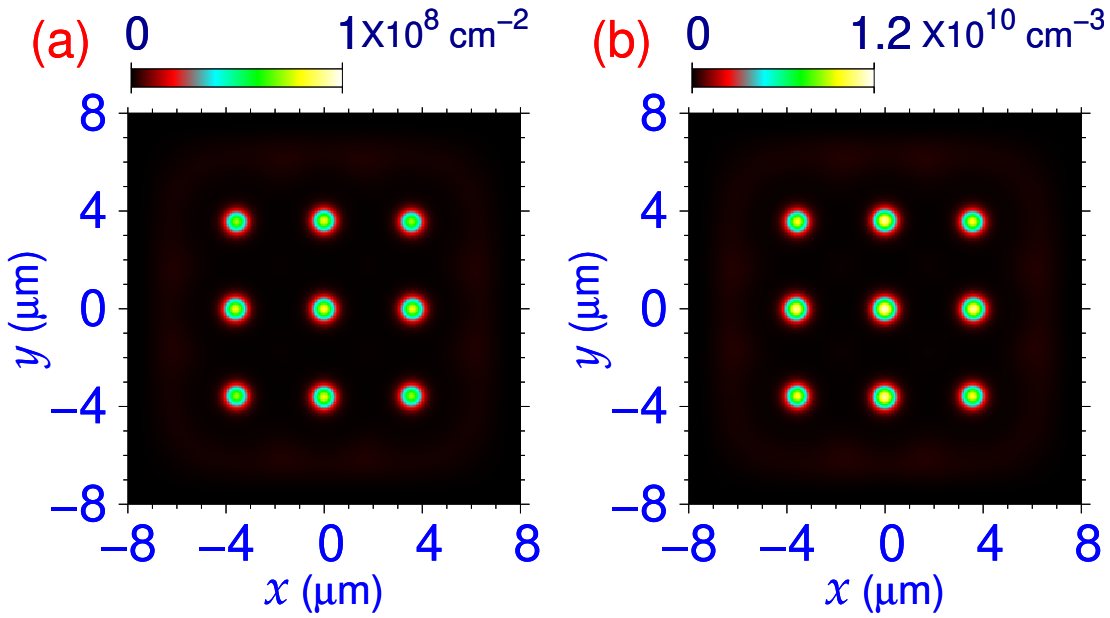

Figure 3: (a) Contour plot of integrated quasi-2D density $n(x, y)$ of a dipolar BEC of $N = 80000$ ^{164}Dy atoms in a trap of angular frequencies $\{\omega_x, \omega_y, \omega_z\} = 2\pi\{33, 33, 167\}$ Hz obrained by imaginary-time propagation. (b) The same by real-time propagation at time $t = 10$ ms, using the converged imaginary-time wave function as the initial state. Atomic scattering (dipolar) length $a = 85a_0$ ($a_{\rm dd} = 130.8a_0$).

the chemical potential values from the current and previous steps.

In the previous programs, initial wave function was initialized as a Gaussian whose values were determined from trap potentials $\gamma = \frac{\omega_x}{\omega_r}$, $\lambda = \frac{\omega_y}{\omega_r}$, $\nu = \frac{\omega_z}{\omega_r}$ with $\psi(x, y, z) \propto \exp\left(-0.5\left(\gamma x^2 + \lambda y^2 + \nu z^2\right)\right)$. In our case, since for the existence of the quantum droplet, potential trap is not necessary, we have added specific, user given, values s_x, s_y and s_z so that the wave function is $\psi(x, y, z) \propto \exp\left(-0.25\left(\frac{x^2}{s_x^2} + \frac{y^2}{s_y^2} + \frac{z^2}{s_z^2}\right)\right)$. What is also changed compared to the previous programs is the way discretization steps dx, dy, dz and dt are initialized. In previous programs they needed to be initialized directly, and in our programs, if they are not initialized, they will be calculated based on the number of points N_x, N_y and N_z and Gaussian variables s_x, s_y and s_z as

$$di = \frac{2s_i m_i}{Ni}, \; dt = \frac{dj^2}{m_t}, \tag{3}$$

where $i \in \{x, y, z\}$, j corresponds to the index of the smallest value between dx, dy or dz and mx, my, mz are also user given variables that determine how big the condensate should be compared to the simulation box (for example, $m_x = m_y = m_z = 10$ menas that the condensate will be 10 times smaller then the simulation box), and m_t determines the time step.

The new programs keep the same names as in previous C CUDA versions: "imag3d-cuda" for imaginary time propagation and "real3d-cuda" for real-time propagation. The program structure, including method names, remains unchanged. The array initialization has been modified to utilize the C++ standard *vector* library, which automatically manages memory, removing the need for manual deallocation.

In the previous programs, the POTMEM setting was used to optimize GPU memory usage. This setting either allocated two tensors for the trap and dipolar potentials or a single tensor with asynchronous copying from main memory when needed. Now, we have introduced a new setting INITIALIZE_POT which has values 0 or 1, where if the first value is chosen, the program will compute trap potential values on-the-fly on the GPU, and if the second value is chosen, the program will create a 3D tensor which it will use to store precomputed values of the trap potential on the GPU. In the FFT section where the CUDA cuFFT library [21] is used, a single tensor contains both the squared wave function and the FFT result. Methods like calcnu, calclux, calcluy, calcluz, and calcnorm all reuse the same temporary array during calculations. Once data is transferred to the GPU, it remains there, and during each time step, physical quantities such as the wave function and densities are copied back to the CPU for display. Additionally, we used the OpenMP library to parallelize loops during the initialization of the wave function, trap potential, and dipolar potential to further enhance performance.

The code's performance was assessed using two GPUs: the consumer-level NVIDIA GTX 1660s and the HPC-optimized NVIDIA A30. Figure 4 displays the speedup in execution time relative to the previous program versions. Tests were conducted on linear grid sizes ranging from 128^3 up to the grid sizes that are close to the maximum that could fit into each GPU's memory - 416^3 for the GTX 1660s with 6 GB and 704^3 for the A30 with 24 GB. Solid lines indicate the average speedup, which is 1.6 for the GTX 1660s and 1.3 for the A30, observed in both the imag3d-cuda (Figure 4a) and relas3d-cuda (Figure 4b) programs.

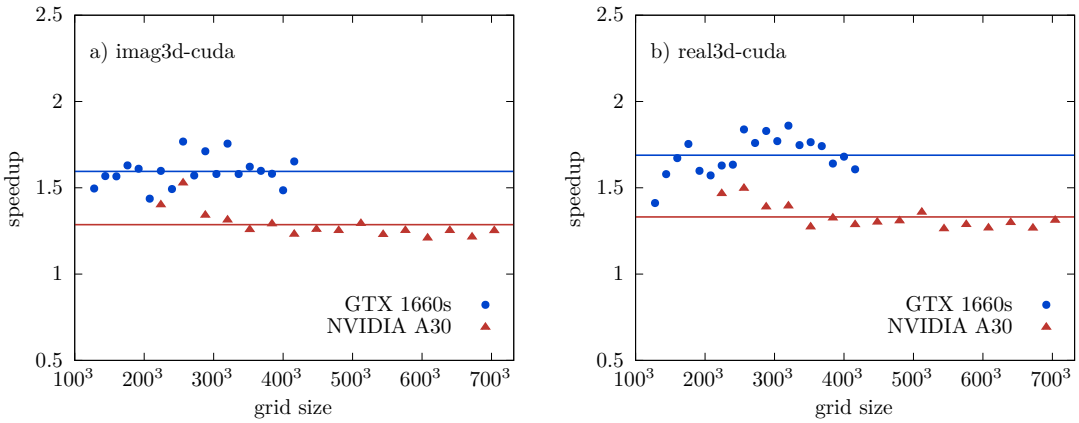

Figure 4: Speedup in execution times of imag3d-cuda and real3d-cuda compared to earlier versions of the programs on NVIDIA GTX 1660 Super and A30 cards. Solid lines show the average speedup achieved. We tested linear grid sizes starting from 128^3 up to the grid sizes that are close to the maximum that could fit into each GPU's memory, which was 416^3 for the GTX 1660 Super and 704^3 for the A30.

The performance of the programs is also evaluated by comparing them to previously published OpenMP/MPI-parallelized programs running on 128 Intel Xeon Gold 6338 CPUs with 128 GB of RAM. The main purpose of this comparison was to assess the potential performance gains from a single GPU card versus an HPC cluster environment. Figure 5 illustrates the speedup of imag3d-cuda and real3d-cuda when run on an NVIDIA A30 card and in a cluster environment. As shown, depending on the grid size, the speedup for imag3d-cuda is three or higher, while for real3d-cuda, it is five or higher.

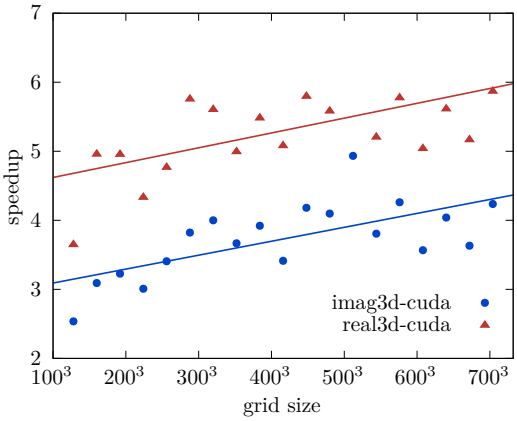

Figure 5: Speedup in execution times of imag3d-cuda and real3d-cuda on NVIDIA A30 card compared to the equivalent MPI/OpenMP parallelized versions of the programs on 128 Intel Xeon Gold 6338 CPUs with 128 GB of RAM. Solid lines show the average speedup achieved.

References

[1] V. Lončar, A. Balaž, A. Bogojević, S. Škrbić, P. Muruganandam, S. K. Adhikari, CUDA programs for solving the time-dependent dipolar Gross-Pitaevskii equation in an anisotropic trap, Computer Physics Communications **200** (2016) 406–410. doi:10.1016/j.cpc.2015.11.014.

[2] A. R. P. Lima, A. Pelster, Beyond mean-field low-lying excitations of dipolar Bose gases, Physical Review A **86** (2012) 063609. doi:10.1103/PhysRevA.86.063609.

[3] A. R. P. Lima, A. Pelster, Quantum fluctuations in dipolar Bose gases, Physical Review A **84** (2011) 041604. doi:10.1103/PhysRevA.84.041604.

[4] F. Wächtler, L. Santos, Quantum filaments in dipolar Bose-Einstein condensates, Physical Review A **93** (2016) 061603. doi:10.1103/PhysRevA.93.061603. arXiv:1601.04501.

[5] H. Kadau, M. Schmitt, M. Wenzel, C. Wink, T. Maier, I. Ferrier-Barbut, T. Pfau, Observing the Rosensweig instability of a quantum ferrofluid, Nature **530** (2016) 194–197. doi:10.1038/nature16485.

[6] I. Ferrier-Barbut, H. Kadau, M. Schmitt, M. Wenzel, T. Pfau, Observation of Quantum Droplets in a Strongly Dipolar Bose Gas, Physical Review Letters **116** (2016) 215301. doi:10.1103/PhysRevLett.116.215301.

[7] P. Muruganandam, S. K. Adhikari, Fortran programs for the time-dependent Gross-Pitaevskii equation in a fully anisotropic trap, Computer Physics Communications **180** (2009) 1888–1912. doi:10.1016/j.cpc.2009.04.015.

[8] R. K. Kumar, L. E. Young-S., D. Vudragović, A. Balaž, P. Muruganandam, S. K. Adhikari, Fortran and C programs for the time-dependent dipolar Gross-Pitaevskii equation in an anisotropic trap, Computer Physics Communications **195** (2015) 117–128. doi:10.1016/j.cpc.2015.03.024. arXiv:1506.03283.

[9] S. K. Adhikari, Bright dipolar Bose-Einstein-condensate soliton mobile in a direction perpendicular to polarization, Physical Review A **90** (2014) 055601. doi:10.1103/PhysRevA.90.055601. arXiv:1410.1369.

[10] S. K. Adhikari, Stable matter-wave solitons in the vortex core of a uniform condensate, Journal of Physics B Atomic Molecular Physics **48** (2015) 165303. doi:10.1088/0953-4075/48/16/165303. arXiv:1506.06367.

[11] S. K. Adhikari, Stable spatial and spatiotemporal optical soliton in the core of an optical vortex, Physical Review E **92** (2015) 042926. doi:10.1103/PhysRevE.92.042926. arXiv:1510.03663.

[12] H. Al-Jibbouri, I. Vidanović, A. Balaž, A. Pelster, Geometric resonances in Bose-Einstein condensates with two- and three-body interactions, Journal of Physics B Atomic Molecular Physics **46** (2013) 065303. doi:10.1088/0953-4075/46/6/065303. arXiv:1208.0991.

[13] J. Akram, A. Pelster, Sculpting quasi-one-dimensional Bose-Einstein condensate to generate calibrated matter waves, Physical Review A **93** (2016) 023606. doi:10.1103/PhysRevA.93.023606. arXiv:1509.03826.

[14] T. Khellil, A. Balaž, A. Pelster, Analytical and numerical study of dirty bosons in a quasi-one-dimensional harmonic trap, New Journal of Physics **18** (2016) 063003. doi:10.1088/1367-2630/18/6/063003. arXiv:1510.04985.

[15] I. Vasić, A. Balaž, Excitation spectra of a Bose-Einstein condensate with an angular spin-orbit coupling, Physical Review A **94** (2016) 033627. doi:10.1103/PhysRevA.94.033627. arXiv:1602.03538.

[16] C.-Y. Lai, C.-C. Chien, Geometry-Induced Memory Effects in Isolated Quantum Systems: Cold-Atom Applications, Physical Review Applied **5** (2016) 034001. doi:10.1103/PhysRevApplied.5.034001. arXiv:1510.08978.

[17] P. Das, P. K. Panigrahi, Controlled generation of nonlinear resonances through sinusoidal lattice modes in Bose-Einstein condensate, Laser Physics **25** (2015) 125501. doi:10.1088/1054-660X/25/12/125501. arXiv:1506.00795.

[18] V. Lončar, L. E. Young-S., S. Škrbić, P. Muruganandam, S. K. Adhikari, A. Balaž, OpenMP, OpenMP/MPI, and CUDA/MPI C programs for solving the time-dependent dipolar Gross-Pitaevskii equation, Computer Physics Communications **209** (2016) 190–196. doi:10.1016/j.cpc.2016.07.029. arXiv:1610.05329.

[19] F. Böttcher, J.-N. Schmidt, J. Hertkorn, K. S. H. Ng, S. D. Graham, M. Guo, T. Langen, T. Pfau, New states of matter with fine-tuned interactions: quantum droplets and dipolar supersolids, Reports on Progress in Physics **84** (2021) 012403. doi:10.1088/1361-6633/abc9ab.

[20] Y. Xiong, L. Yin, Effective single-mode model of a binary boson mixture in the quantum droplet region, Physical Review A **105** (2022) 053305. doi:10.1103/PhysRevA.105.053305.

[21] cuFFT, CUDA API References, CUDA Toolkit Documentation v13.0, 2025. URL: https://docs.nvidia.com/cuda/cufft.